Letter

Theory of Coulomb excitation of the ^{229}Th nucleus by protons

Tao Li,[1] Hanxu Zhang,[1] and Xu Wang[1,2,*]

[1]*Graduate School, China Academy of Engineering Physics, Beijing 100193, China*

[2]*Southern Center for Nuclear-Science Theory, Institute of Modern Physics, Chinese Academy of Sciences, Huizhou, Guangdong 516000, China*

(Received 11 April 2023; accepted 3 October 2023; published 13 October 2023)

One of the current research focuses on ^{229}Th is to search for efficient methods to excite the nucleus from the ground state to the low-lying isomeric state. While existing methods are either optical or electronic excitation, we propose herein to use Coulomb excitation by protons for producing the isomer. A theoretical framework is developed for the protonic Coulomb excitation process, and the isomeric excitation cross section is calculated to be over 10 mb with a typical proton energy of 10 MeV. Proton excitation is particularly advantageous for solid-state targets owing to its strong penetrability through materials, and its experimental implementation is relatively straightforward. An experimental scheme featuring ^{229}Th-doped crystals is envisaged, and an assessment of the expected excitation efficiency is provided.

DOI: 10.1103/PhysRevC.108.L041602

Introduction. The ^{229}Th nucleus is unique in nuclear physics, as it hosts an extremely low-lying isomeric state of energy approximately 8 eV [1–6]. This isomeric state, denoted ^{229m}Th, offers great potential for various applications, including nuclear optical clocks [7–9], nuclear lasers [10], checking variations of fundamental constants [11–13], etc.

The current workhorse of producing ^{229m}Th is α decay of ^{233}U [14,15]. Due to the long decay lifetime (1.6×10^5 yr) and the low branching ratio to the isomeric state (2%), the efficiency is rather low. Besides, the resultant ^{229}Th nuclei have an undesired recoil energy of 84 keV into random directions. Alternatively, ^{229m}Th may be obtained from β decay of ^{229}Ac [16]. This scheme has been applied in a recent work yielding improved accuracy of the isomeric energy [17].

One of the current focuses of research is to identify efficient *active* excitation methods for the ^{229}Th nucleus. Several methods have been proposed and explored, including: (1) Direct optical excitation using vacuum-ultraviolet (VUV) light around 8 eV, though experimental attempts have yet to produce positive results [18–21]. (2) Indirect optical excitation utilizing 29-keV synchrotron radiation, where the nucleus is pumped from the ground state to the second excited state, which subsequently decays into the isomeric state [22]. This approach has been experimentally demonstrated in [23]. (3) Excitation via electronic-bridge processes, which has been proposed for several systems [24–30], but experimental realizations have not yet been reported. (4) Excitation by inelastic electron scattering, which is most efficient for low-energy electrons around 10 eV, and the corresponding cross sections are on the order of 1 mb [31,32]. (5) Excitation in laser-generated plasmas [33], which has been experimentally demonstrated in [34]. (6) Excitation by strong femtosecond laser pulses via electron recollision [35–38]. (7) Excitation in laser-heated clusters [39].

The summary presented above indicates that the existing methods are either optical excitation (methods 1–2) or (laser-driven) electronic excitation (methods 3–7). While optical excitation (methods 1–2) and electronic-bridge excitation (method 3) are appropriate for solid-state experiments, the resonant condition requires strict fulfillment, which is difficult to achieve due to current uncertainties regarding both nuclear and electronic levels. That partly explains the current status that only the indirect optical excitation method (method 2) has been demonstrated experimentally, which nevertheless necessitates narrow-band synchrotron radiation around 29 keV and photon-energy scanning for nuclear resonance [23]. In contrast, electronic excitations (methods 4–7) do not require a resonant condition. However, these methods are better suited for gas or plasma experiments [34], as low-energy electrons around 10 eV are most efficient for the isomeric excitation [31,32], but these electrons have very limited penetrability (approximately 1 nm) through solid-state materials [40,41].

In this Letter, we propose an approach to use protons for the isomeric excitation. We investigate the Coulomb excitation of the ^{229}Th nucleus by a proton beam and develop a theoretical framework to compute the isomeric excitation cross section. Proton excitation offers a unique combination of advantages: (1) Promising excitation cross sections. Calculations show that the isomeric excitation cross section is over 10 mb with a typical proton energy of 10 MeV. (2) Strong penetrability through solid-state materials, making it well suited for solid-state experiments. Protons have a penetration depth on the order of 0.1–1 mm [42,43]. (3) No precise knowledge of the isomeric energy or resonant condition is required. (4) Straightforward and relatively simple experimental implementation. Proton excitation combines the benefits of

*Corresponding author: xwang@gscaep.ac.cn

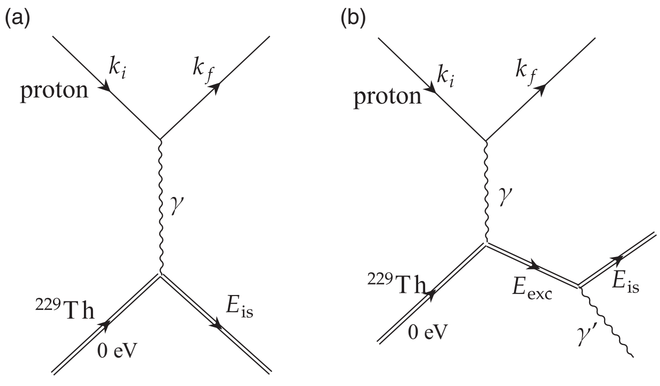

FIG. 1. Illustration of isomeric excitation of the ^{229}Th nucleus by protons. (a) An incident proton excites the ^{229}Th nucleus from the ground state to the isomeric state (with energy E_{is}) via exchanging a virtual photon. (b) An incident proton excites the ^{229}Th nucleus from the ground state to a higher excited state (with energy E_{exc}) which then decays into the isomeric state.

optical and electronic excitation methods from the perspective of solid-state experiments.

Coulomb excitation by protons and the excitation cross section. The mechanism of isomeric excitation by protons can be visualized by two Feynman diagrams as depicted in Fig. 1. In diagram (a), the incident proton transfers energy via a virtual photon to the ^{229}Th nucleus, exciting it to the isomeric state. (The isomeric energy E_{is} is taken to be 8.28 eV [5] in this Letter, but our results are rather insensitive to a change of this energy on the order of 0.1 eV [6,17].) If the proton energy exceeds about 29 keV, which is the energy of the second excited state, diagram (b) is open in addition, in which the ^{229}Th nucleus is excited to a higher excited state with energy E_{exc}. The excited state then decays rapidly, typically within a lifetime of 10–100 ps, (directly or successively) into the isomeric state with some probability (i.e. branching ratio). For proton energies around 10 MeV, multiple higher excited states have to be considered, as listed below.

The system under consideration contains three parts: the ^{229}Th nucleus (Hamiltonian denoted H_{n}), the proton (H_{p}), and the radiation field (H_{r}). The total Hamiltonian of the system is

$$H = H_{\mathrm{n}} + H_{\mathrm{p}} + H_{\mathrm{r}} + H_{\mathrm{int}}, \tag{1}$$

where the interaction Hamiltonian is given by [44]

$$H_{\mathrm{int}} = -\frac{1}{c}\int d^3\mathbf{r}\,[\mathbf{j}_{\mathrm{n}}(\mathbf{r})\cdot\mathbf{A}(\mathbf{r}) + \mathbf{j}_{\mathrm{p}}(\mathbf{r})\cdot\mathbf{A}(\mathbf{r})] + \int d^3\mathbf{r}d^3\mathbf{r}'\,\frac{\rho_{\mathrm{n}}(\mathbf{r})\rho_{\mathrm{p}}(\mathbf{r}')}{|\mathbf{r}-\mathbf{r}'|}. \tag{2}$$

Here, c is the speed of light, $\mathbf{j}_{\mathrm{n/p}}$, $\rho_{\mathrm{n/p}}$ are the current density and the charge density operator for the nucleus or the proton. $\mathbf{A}(\mathbf{r})$ is the vector potential of the radiation field, which can be expanded into electric (E) and magnetic (M) multipole components [45]

$$\mathbf{A}(\mathbf{r}) = \sum_{\lambda,\mu,q}[a(E\lambda,\mu,q)\mathbf{A}(E\lambda,\mu,q) + a(M\lambda,\mu,q)\mathbf{A}(M\lambda,\mu,q)] + \mathrm{H.c.} \tag{3}$$

with the multipole fields given by

$$\mathbf{A}(M\lambda,\mu,q) = \sqrt{\frac{8\pi c^2 q^2}{\lambda(\lambda+1)R}}\mathbf{L}[j_\lambda(qr)\mathrm{Y}_{\lambda\mu}(\theta,\phi)], \tag{4}$$

$$\mathbf{A}(E\lambda,\mu,q) = \nabla\times\mathbf{A}(M\lambda,\mu,q). \tag{5}$$

In the above expressions λ, μ, q are, respectively, the angular momentum quantum number, the magnetic quantum number, and the wave number of the photon. R is the radius of the quantization volume. $\mathbf{L} = -i\mathbf{r}\times\nabla$ is the angular momentum operator, $j_\lambda(qr)$ is a spherical Bessel function, and $\mathrm{Y}_{\lambda\mu}(\theta,\phi)$ is a spherical harmonic function. The expansion coefficient a and its conjugate are photon annihilation and creation operators with matrix elements $\langle n|a|n+1\rangle = \sqrt{(n+1)/2qc}$, where $|n\rangle$ represents an n-photon number state in the mode specified by a.

The initial and final states of the system are product of the three parts: $|i\rangle = |I_iM_i\rangle\otimes|\psi_i\rangle\otimes|0\rangle$ and $|f\rangle = |I_fM_f\rangle\otimes|\psi_f\rangle\otimes|0\rangle$, where I and M represent the total angular momentum and magnetic quantum number of the nuclear state, $|\psi_{i/f}\rangle$ denotes the proton state, and $|0\rangle$ means the photon vacuum. The transition matrix element can be derived into the following form:

$$\langle f|H_{\mathrm{int}}|i\rangle = \sum_{\lambda,\mu}\frac{4\pi}{2\lambda+1}(-1)^\mu \times [\langle I_fM_f|\mathcal{M}(E\lambda,-\mu)|I_iM_i\rangle\langle\psi_f|\mathcal{N}(E\lambda,\mu)|\psi_i\rangle - \langle I_fM_f|\mathcal{M}(M\lambda,-\mu)|I_iM_i\rangle\langle\psi_f|\mathcal{N}(M\lambda,\mu)|\psi_i\rangle], \tag{6}$$

where $\mathcal{M}$ and $\mathcal{N}$ are multipole transition operators [44] for the nucleus and for the proton, respectively. The nuclear excitation cross section is

$$\sigma = \int d\Omega_f\frac{E_iE_f}{4\pi^2c^4}\frac{p_f}{p_i}\frac{1}{2(2I_i+1)}\sum_{M_i,M_f}\sum_{\nu_i,\nu_f}|\langle f|H_{\mathrm{int}}|i\rangle|^2, \tag{7}$$

where Ω_f is the solid angle of the outgoing proton, $E_{i,f}$, $p_{i,f}$ are the energy and momentum of the initial or the final state of the proton, $M_{i,f}$ is the magnetic quantum number of the initial or the final nuclear state, and $\nu_{i,f}$ is the proton spin for the initial or the final state.

By introducing reduced nuclear transition probabilities

$$B(\mathcal{T}\lambda;I_i\to I_f) = \frac{1}{2I_i+1}\sum_{M_f,M_i,\mu}|\langle I_fM_f|\mathcal{M}(\mathcal{T}\lambda,\mu)|I_iM_i\rangle|^2, \tag{8}$$

where $\mathcal{T}$ can be either E or M, the nuclear excitation cross section can be written in the following form:

$$\sigma = \int d\Omega_f\frac{4E_iE_f}{c^4}\frac{p_f}{p_i}\sum_{\lambda,\mathcal{T},\mu}\frac{B(\mathcal{T}\lambda;I_i\to I_f)}{2(2\lambda+1)^3} \times\sum_{\nu_i,\nu_f}|\langle\psi_f|\mathcal{N}(\mathcal{T}\lambda,\mu)|\psi_i\rangle|^2. \tag{9}$$

The desired feature of the above expression is that the nuclear information is packed in the reduced transition probability

TABLE I. Important nuclear excited states of ^{229}Th in proton-induced isomeric excitation.

Energy level (keV)[a]	I_e^π	$\mathcal{T}\lambda$	$B(\mathcal{T}\lambda, e \to g)$[b]	ratio decaying into ^{229m}Th (%)[c]
0.008	$3/2^+$	$E2; M1$	0.225; 0.0136	100
29.18	$5/2^+$	$E2; M1$	3.0; 0.0041	58
42.34	$7/2^+$	$E2; M1$	2.3; 0.018	5.9
71.82	$7/2^+$	$E2; M1$	0.018; 0.001	59
97.14	$9/2^+$	$E2$	0.86	20
125.51	$9/2^+$	$E2$	0.32	72
320.55	$5/2^+$	$E2; M1$	0.15; 0.0057	46

[a]Data in this table are taken from Refs. [50–53].
[b]Reduced transition probabilities to the ground state, in the unit of $e^2\mathrm{b}^2$ for $E2$ and μ_N^2 for $M1$.
[c]Calculated by considering all cascade decays, including γ decays and IC decays.

B and the proton information is packed in the matrix element of $\mathcal{N}$.

The proton wave functions $\psi_{i,f}$ are obtained by solving the time-independent Dirac equation

$$[-ic\boldsymbol{\alpha} \cdot \nabla + \beta c^2 + V_{\mathrm{Th}}(r)]\psi_{i,f} = E_{i,f}\psi_{i,f}, \qquad (10)$$

where $\boldsymbol{\alpha} = \{\alpha_1, \alpha_2, \alpha_3\}$ and β are 4×4 matrices, and $V_{\mathrm{Th}}(r)$ is the potential felt by the proton from the ^{229}Th atom or ion. In our calculation, a Dirac-Hartree-Fock-Slater method [46,47] is used to calculate the charge distribution of the ^{229}Th atom or ion and to obtain the potential $V_{\mathrm{Th}}(r)$. The nuclear charge density is described by a Fermi distribution [48]. The openly accessible code RADIAL [49] is used to calculate the wave function of the proton, i.e., numerically solving the above Dirac equation.

A proton beam has typical energies on the order of 1–10 MeV, so the ^{229}Th nucleus can be excited to both the isomeric state and higher excited states. The higher excited states have very short lifetimes on the order of 10–100 ps [50–53] (the 8-eV state is the only known isomeric state of ^{229}Th), and they decay, directly or successively, into the ground state and the isomeric state. The isomeric state has a lifetime on the order of 10^3 s via γ decay [34] or 10^{-6} s via internal conversion (IC) [54]. In real experiments, one would find ways to prevent the IC process in order to maintain the isomeric state, as discussed below. So the lifetime of the isomeric state can be taken as the γ-decay lifetime, which is at least 13 orders of magnitude longer than those of higher excited states. It is therefore meaningful, for excitation times shorter than the 10^3-s lifetime, to define an effective isomeric excitation cross section taking into account of all higher excited states and the corresponding branching ratio decaying into the isomeric state:

$$\sigma_{\mathrm{eff}}(E_i) = \sum_n r_n \sigma_n(E_i), \qquad (11)$$

where n designates a particular excited state, $\sigma_n(E_i)$ is the excitation cross section from the ground state to this excited state, and r_n is the branching ratio of this excited state decaying into the isomeric state. The above formula should also include the direct excitation channel to the isomeric state, for which we just put the branching ratio to be 100%. The summation is taken over nuclear excited states with energies smaller than the proton incoming energy E_i.

The effective excitation cross section σ_{eff} as well as cross sections of individual excited states σ_n are displayed in Fig. 2. Only a few excited states contribute significantly to σ_{eff}, and the information of these states is listed in Table I. Other unlisted states either have little contribution (below the vertical range shown in Fig. 2) or lack data on the reduced nuclear transition probabilities. The value of σ_{eff} is approximately 1 mb for proton energy 1 MeV, and 15 mb for 10 MeV. For proton energies below 0.2 MeV, the dominant contributor to σ_{eff} is the 8.28-eV direct-excitation channel. With higher energies, several other channels surpass the direct channel. At energies around 10 MeV, the 29-keV state and the 42-keV state have similar excitation cross sections, but the former channel contributes more to σ_{eff} because its branching ratio decaying into the isomeric state is about 10 times higher than the latter channel.

The dependency of the cross sections on the ionic state is rather weak: the neutral Th atom and the bare Th^{90+} ion lead to visually indistinguishable cross-section curves, at least for

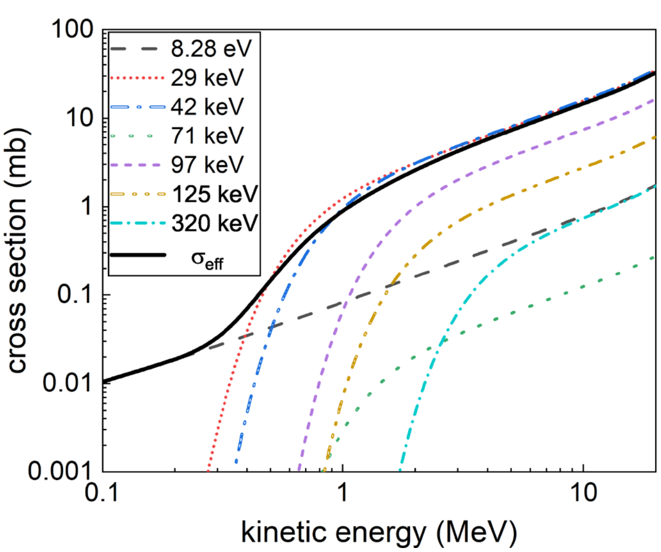

FIG. 2. Coulomb excitation cross sections by protons. The (black) solid curve is the effective isomeric excitation cross section calculated using Eq. (11). The dashed curves show the nuclear excitation cross sections from the ground state to different excited states, the information of which is listed in Table I.

the energy range shown in Fig. 2. This is understandable, since the disturbance of the electron cloud on the proton is on the order of 1–10 keV, much smaller than the energy of the proton itself.

Discussion. (a) Applicability of the current theory. In this work the mechanism of Coulomb excitation is considered. If the energy is high, the proton may penetrate into the ^{229}Th nucleus and initiate nuclear reactions, which are beyond the scope of the current Letter. It is worth noting that Coulomb excitation can still be detected even if the cross section for compound nucleus formation surpasses it, as the compound nucleus typically decays mainly into other channels besides the one corresponding to inelastic scattering [44].

We have checked the wave function of the proton for each incoming energy, and found that the portion of the wave function inside the ^{229}Th nuclear radius ($\approx$7.3 fm using the formula $r = r_0 A^{1/3}$ with $r_0 = 1.2$ fm) is negligible for energies below about 20 MeV. This is consistent to a rough classical estimation based on equating the closest head-on-collision distance to the nuclear radius, which yields an energy of approximately 18 MeV. Consequently, Coulomb excitation is expected to be the dominant excitation mechanism for proton energies below about 20 MeV. This is the energy range shown in Fig. 2. For proton energies above 20 MeV, additional studies are required to determine the relative contributions of Coulomb excitation and strong-interaction excitation.

(b) Comparison with electron excitation. The latter has been studied in detail in [31,32]. While both excitations share the same underlying mechanism of Coulomb excitation, they exhibit very different behavior due to the repulsive or attractive nature of the interaction. Low-energy electrons at around 10 eV have been found to be most efficient for the isomeric excitation, resulting in excitation cross sections on the order of 1 mb. However, the cross section drops as the electron energy increases. In contrast, the cross section for proton excitation increases with increasing proton energy (Fig. 2). Low-energy electrons have poor penetrability through solid-state targets, making electron excitation more suitable for gas or plasma experiments [34], while proton excitation is ideal for solid-state experiments.

(c) Experimental considerations. For a solid-state target, the IC process can be blocked by doping ^{229}Th ions into VUV-transparent crystals with band gaps larger than the isomeric energy. Several crystals, such as $LiCaAlF_6$ [8], SiO_2 [34], CaF_2 [30], LiF [55], have been employed or proposed for this purpose. It has been demonstrated experimentally that the density of the doped Th ions can be higher than 10^{18} cm^{-3} [8].

We consider exposing a ^{229}Th-doped crystal (e.g., the CaF_2 crystal, but our discussions apply similarly to other crystals as well) to a proton beam, as illustrated in Fig. 3. The size of proton beams are typically on the order of 1 cm [56], and we assume the area of the sample to be 1 cm^2. We consider a typical proton energy of 10 MeV, and we use the SRIM (Stopping and Range of Ions in Matter) software [43] to calculate the residual energy of the protons as they penetrate the CaF_2 crystal, as shown in Fig. 3. The protons can travel a maximum distance of about 0.5 mm into the crystal. We assume the sample thickness to be 0.1 mm, and the protons

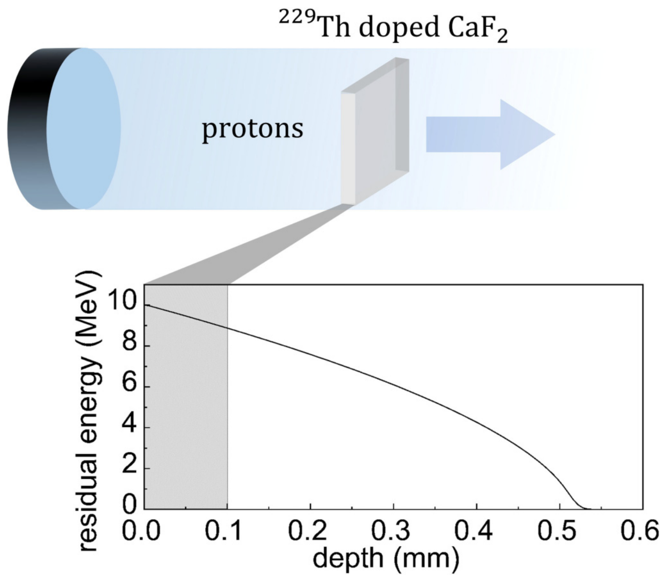

FIG. 3. Schematic illustration of the envisaged experiment. A ^{229}Th-doped CaF_2 crystal is exposed to a proton beam of energy 10 MeV. The lower image shows the residual energy of the proton beam as it penetrates this crystal, calculated using the SRIM software. If the sample thickness is 0.1 mm, the proton beam can pass through the sample without significant energy loss.

can pass through this thickness without losing much energy. The volume of the sample is then 10^{-2} cm^3.

From Fig. 2 we know that the isomeric excitation cross section $\sigma_{\rm eff} \approx 15$ mb. Assuming a typical charge current of 10 μA passing through the sample, the proton flux density $j = 6.24 \times 10^{13}$ s^{-1} cm^{-2}. Then the isomeric excitation rate per nucleus is $\Gamma = j\sigma_{\rm eff} \approx 10^{-12}$ s^{-1}. The total number of ^{229}Th ions within the sample is approximately $N \approx 10^{18}$ cm^{-3} $\times$ 10^{-2} cm$^3 = 10^{16}$. Hence, the production rate of ^{229m}Th is about 10^4 s^{-1}. For a proton irradiation time of 100 s, the number of generated ^{229m}Th nuclei will be 10^6. After the proton irradiation, these nuclei will decay and emit photons around 8 eV within the lifetime of 10^3 s. Therefore, approximately 10^3 VUV photons will be emitted per second, which is detectable with modern photon detectors.

The proton irradiation dose is ultimately limited by the defects created by the protons. Too many defects may lower the band gap [57–59] and reopen the IC process which de-excites the generated isomeric state. We have found no systematic work studying the effect of proton irradiation on the band gap of thorium-doped crystals. Nevertheless, an estimation of this effect can be made via calculating the number of proton-induced vacancies using the SRIM software. For the proton irradiation dose that we use above (10 μA for 100 s), the density of vacancies is calculated to be 10^{18} cm^{-3}, which is 5 orders of magnitude lower than the density of all ions (see the Supplemental Material [60] for details). That is, for each generated ^{229m}Th, the probability of a point defect nearby is about 10^{-5}. From this estimation we postulate that proton-induced defects are not severe for such an irradiation dose. Besides, thermal annealing effects, which are not taken into account in SRIM, tend to reduce the number of defects further [62].

Existing experimental results indeed show low concentration of defects in proton-irradiated CaF_2 single crystals [60,63]. Of course, systematic investigations from computational materials science are desirable to determine the optimal proton irradiation dose.

(d) The possibility of using Coulomb excitation to obtain ^{229m}Th is briefly mentioned in Refs. [64,65]. Isakov calculated this process based on a classical Coulomb excitation theory [44] and obtained an effective excitation cross section about an order of magnitude lower than our results [66]. The difference is mainly due to the usage of different values of the nuclear reduced transition probabilities, especially between the ground state and the 29-keV excited state. Isakov used a theoretically determined value, whereas we use a new experimental value [52]. We have checked that if we adopt the same nuclear transition probabilities, we obtain results close to Isakov's [e.g., for proton energy 10 MeV, $\sigma(8\ \text{eV}) = 0.238$ mb in comparison to 0.231 mb from Isakov, and $\sigma(29\ \text{keV}) = 0.355$ mb in comparison to 0.346 mb from Isakov]. This indicates that the classical theory is quite adequate for the current situation. Nevertheless, the classical results may deviate substantially from the quantum results in other situations, and a careful benchmark is desirable.

(e) Last, we mention that the excitation theory developed in this Letter can also be applied to other positive projectiles, such as α particles or even heavier nuclei or ions, with minor modifications of parameters (see the Supplemental Material for an example [60]).

Conclusion. In summary, we propose an efficient approach for the isomeric excitation of ^{229}Th using protons. A theoretical framework is developed for the Coulomb excitation of the ^{229}Th nucleus by a proton beam, and the excitation cross section is calculated. With a typical proton energy of 10 MeV, the effective excitation cross section from the ground state to the low-lying isomeric state is calculated to be exceeding 10 mb. A potential experimental realization is envisaged using ^{229}Th-doped crystals and the excitation efficiency is estimated. Notably, this method does not require precise knowledge of the isomeric energy or resonant conditions, and it is well-suited for solid-state experiments. With proton beams being readily accessible worldwide, we anticipate that experimental realization of this approach is feasible and can advance the study of the ^{229}Th nuclear isomer.

Acknowledgments. We acknowledge helpful discussions with Mr. Huaqing Huang from Peking University, Mr. Shenghong Wang from Lanzhou University, and Prof. Pengfei Guan from Beijing CSRC. This work was supported by NSAF Grant No. U2330401 and NSFC Grant No. 12088101.

T.L. and H.Z. contributed equally to this work.

[1] L. A. Kroger and C. W. Reich, Nucl. Phys. A **259**, 29 (1976).
[2] C. W. Reich and R. G. Helmer, Phys. Rev. Lett. **64**, 271 (1990).
[3] R. G. Helmer and C. W. Reich, Phys. Rev. C **49**, 1845 (1994).
[4] B. R. Beck, J. A. Becker, P. Beiersdorfer, G. V. Brown, K. J. Moody, J. B. Wilhelmy, F. S. Porter, C. A. Kilbourne, and R. L. Kelley, Phys. Rev. Lett. **98**, 142501 (2007).
[5] B. Seiferle *et al.*, Nature (London) **573**, 243 (2019).
[6] E. Peik, T. Schumm, M. S. Safronova, A. Pálffy, J. Weitenberg, and P. G. Thirolf, Quantum Sci. Technol. **6**, 034002 (2021).
[7] E. Peik and C. Tamm, Europhys. Lett. **61**, 181 (2003).
[8] W. G. Rellergert, D. DeMille, R. R. Greco, M. P. Hehlen, J. R. Torgerson, and E. R. Hudson, Phys. Rev. Lett. **104**, 200802 (2010).
[9] C. J. Campbell, A. G. Radnaev, A. Kuzmich, V. A. Dzuba, V. V. Flambaum, and A. Derevianko, Phys. Rev. Lett. **108**, 120802 (2012).
[10] E. V. Tkalya, Phys. Rev. Lett. **106**, 162501 (2011).
[11] V. V. Flambaum, Phys. Rev. Lett. **97**, 092502 (2006).
[12] J. C. Berengut, V. A. Dzuba, V. V. Flambaum, and S. G. Porsev, Phys. Rev. Lett. **102**, 210801 (2009).
[13] P. Fadeev, J. C. Berengut, and V. V. Flambaum, Phys. Rev. A **102**, 052833 (2020).
[14] V. Barci, G. Ardisson, G. Barci-Funel, B. Weiss, O. El Samad, and R. K. Sheline, Phys. Rev. C **68**, 034329 (2003).
[15] J. Thielking, M. V. Okhapkin, P. Głowacki, D. M. Meier, L. Wense, B. Seiferle, C. E. Düllmann, P. G. Thirolf, and E. Peik, Nature (London) **556**, 321 (2018).
[16] M. Verlinde *et al.*, Phys. Rev. C **100**, 024315 (2019).
[17] S. Kraemer *et al.*, Nature (London) **617**, 706 (2023).
[18] J. Jeet, C. Schneider, S. T. Sullivan, W. G. Rellergert, S. Mirzadeh, A. Cassanho, H. P. Jenssen, E. V. Tkalya, and E. R. Hudson, Phys. Rev. Lett. **114**, 253001 (2015).
[19] E. Peik and M. Okhapkin, C. R. Phys. **16**, 516 (2015).
[20] A. Yamaguchi, M. Kolbe, H. Kaser, T. Reichel, A. Gottwald, and E. Peik, New J. Phys. **17**, 053053 (2015).
[21] S. Stellmer, G. Kazakov, M. Schreitl, H. Kaser, M. Kolbe, and T. Schumm, Phys. Rev. A **97**, 062506 (2018).
[22] E. V. Tkalya, A. N. Zherikhin, and V. I. Zhudov, Phys. Rev. C **61**, 064308 (2000).
[23] T. Masuda *et al.*, Nature (London) **573**, 238 (2019).
[24] E. V. Tkalya, JETP Lett. **55**, 212 (1992).
[25] S. G. Porsev and V. V. Flambaum, Phys. Rev. A **81**, 042516 (2010).
[26] S. G. Porsev, V. V. Flambaum, E. Peik, and C. Tamm, Phys. Rev. Lett. **105**, 182501 (2010).
[27] P. V. Bilous, E. Peik, and A. Pálffy, New J. Phys. **20**, 013016 (2018).
[28] A. Y. Dzyublik, Phys. Rev. C **102**, 024604 (2020).
[29] P. V. Bilous, H. Bekker, J. C. Berengut, B. Seiferle, L. von der Wense, P. G. Thirolf, T. Pfeifer, J. R. C. López-Urrutia, and A. Pálffy, Phys. Rev. Lett. **124**, 192502 (2020).
[30] B. S. Nickerson, M. Pimon, P. V. Bilous, J. Gugler, K. Beeks, T. Sikorsky, P. Mohn, T. Schumm, and A. Pálffy, Phys. Rev. Lett. **125**, 032501 (2020).
[31] E. V. Tkalya, Phys. Rev. Lett. **124**, 242501 (2020).
[32] H. Zhang, W. Wang, and X. Wang, Phys. Rev. C **106**, 044604 (2022).
[33] H. Zhang and X. Wang, Front. Phys. **11**, 1166566 (2023).

[34] P. V. Borisyuk, E. V. Chubunova, N. N. Kolachevsky, Yu. Yu. Lebedinskii, O. S. Vasiliev, and E. V. Tkalya, arXiv:1804.00299.

[35] W. Wang, J. Zhou, B. Liu, and X. Wang, Phys. Rev. Lett. **127**, 052501 (2021).

[36] W. Wang, H. Zhang, and X. Wang, J. Phys. B: At. Mol. Opt. Phys. **54**, 244001 (2021).

[37] X. Wang, Phys. Rev. C **106**, 024606 (2022).

[38] W. Wang and X. Wang, arXiv:2306.10686.

[39] J. Qi, H. Zhang, and X. Wang, Phys. Rev. Lett. **130**, 112501 (2023).

[40] J. C. Ashley and V. E. Anderson, J. Electron Spectrosc. Relat. Phenom. **24**, 127 (1981).

[41] Q. Gibaru, C. Inguimbert, M. Belhaj, M. Raine, and D. Lambert, Appl. Surf. Sci. **570**, 151154 (2021).

[42] U. Fano, Annu. Rev. Nucl. Sci. **13**, 1 (1963).

[43] J. F. Ziegler, M. D. Ziegler, and J. P. Biersack, Nucl. Instrum. Methods Phys. Res. B **268**, 1818 (2010).

[44] K. Alder, A. Bohr, T. Huus, B. Mottelson, and A. Winther, Rev. Mod. Phys. **28**, 432 (1956).

[45] J. M. Blatt and V. F. Weisskopf, *Theoretical Nuclear Physics* (John Wiley & Sons, New York, 1952).

[46] D. Liberman, J. T. Waber, and D. T. Cromer, Phys. Rev. **137**, A27 (1965).

[47] D. Liberman, D. T. Cromer, and J. T. Waber, Comput. Phys. Commun. **2**, 107 (1971).

[48] B. Hahn, D. G. Ravenhall, and R. Hofstadter, Phys. Rev. **101**, 1131 (1956).

[49] F. Salvat and J. M. Fernandez-Varea, Comput. Phys. Commun. **240**, 165 (2019).

[50] E. Ruchowska *et al.*, Phys. Rev. C **73**, 044326 (2006).

[51] E. Browne and J. K. Tuli, Nucl. Data Sheets **109**, 2657 (2008).

[52] Y. Shigekawa *et al.*, Phys. Rev. C **104**, 024306 (2021).

[53] N. Minkov and A. Pálffy, Phys. Rev. Lett. **118**, 212501 (2017).

[54] B. Seiferle, L. von der Wense, and P. G. Thirolf, Phys. Rev. Lett. **118**, 042501 (2017).

[55] Q. Gong, C. Zhao, S. Tao, Y. Hang, S. Zhu, and L. Ma, Adv. Opt. Mater. **11**, 2202327 (2023).

[56] H. Shu, C. Yin, H. Zhang, M. Liu, M. Zhang, L. Zhao, K. Chu, X. Dai, and M. F. Moyers, MethodsX **6**, 1933 (2019).

[57] P. Dessovic, P. Mohn, R. A. Jackson, J. Winkler, M. Schreitl, G. Kazakov, and T. Schumm, J. Phys.: Condens. Matter **26**, 105402 (2014).

[58] P. V. Borisyuk, O. S. Vasilyev, A. V. Krasavin, Y. Yu. Lebedinskii, V. I. Troyan, and E. V. Tkalya, Phys. Status Solidi C **12**, 1333 (2015).

[59] K. A. A. G. Beeks, Ph.D. thesis, Technische Universität Wien, Vienna, Austria, 2022.

[60] See Supplemental Material at http://link.aps.org/supplemental/10.1103/PhysRevC.108.L041602 for details of SRIM simulations and an example of α particle-induced Coulomb excitation, which includes Ref. [61].

[61] R. Sherr, C. W. Li, and R. F. Christy, Phys. Rev. **96**, 1258 (1954).

[62] P. C. Hsu and T. K. Wang, Radiat. Prot. Dosim **16**, 253 (1986).

[63] R. Hazem and M. Izerrouken, Radiat. Phys. Chem. **204**, 110643 (2023).

[64] C. E. Bemis *et al.*, Phys. Scr. **38**, 657 (1988).

[65] V. S. Alexandrov *et al.*, Acta Phys. Pol. B **42**, 853 (2011).

[66] V. I. Isakov, Phys. At. Nucl. **80**, 1080 (2017).